Electronic Supplementary Material (ESI) for Nanoscale.

Design of antibody-functionalized carbon nanotubes filled with radioactivable metals towards a targeted anticancer therapy

Cinzia Spinato,[a] Aritz Perez Ruiz de Garibay,[a] Magdalena Kierkowicz,[b] Elzbieta Pach,[c] Markus Martincic,[b] Rebecca Klippstein,[d] Maxime Bourgognon,[d] Julie Tzu-Wen Wang,[d] Cécilia Ménard-Moyon,[a] Khuloud T. Al-Jamal,[d] Belén Ballesteros,[c] Gerard Tobias,[b*] Alberto Bianco[a*]

ELECTRONIC SUPPLEMENTARY INFORMATION

Table of Contents

1. General Methods

The chemicals and solvents were obtained from commercial suppliers and used without further purification. The solvents used for synthesis were analytical grade. When anhydrous conditions were required, high quality commercial dry solvents were used. Water was purified using a Millipore filter system MilliQ®. When stated, suspensions were sonicated in a water bath (20 W, 40 kHz). Thin layer chromatography (TLC) was conducted on pre-coated aluminum plates with 0.25 mm Macherey-Nagel silica gel with fluorescent indicator UV254. Chromatographic purifications were carried out with silica gel (Merck Kieselgel 60, 40-60 μm, 230-400 mesh ASTM). ^{1}H-NMR spectra were recorded in deuterated solvents using Bruker spectrometers (Avance III - 400 MHz and Avance I - 500 MHz). Chemical shifts are reported in ppm using the residual signal of deuterated solvent as reference. The resonance multiplicity is described as *s* (singlet), *t* (triplet), *qt* (quintuplet), *m* (multiplet), *bs* (broad singlet), and *bt* (broad triplet). Coupling constants (*J*) are given in Hz. For CNTs filtration, PTFE membrane from Millipore were employed. If not differently specified, dialysis of CNT compounds was carried out employing a membrane with MWCO 12000-14000 Da, purchased from Spectrum Laboratories, Inc. Mini-dialysis and buffer exchange were performed in Slide-A-Lyzer dialysis tubes (10000 MWCO) from Thermo Scientific. Centrifugation was performed either using an Eppendorf 5804 R apparatus, or on a Beckman Avanti J-25 centrifuge equipped with JS-7.5 rotor. UV-Vis spectroscopy was performed on a Varian Cary 5000 spectrophotometer and the Kaiser test was performed according to reported procedures.[1,2] TGA under flowing air was performed on a TA Instrument Q5000 IR (for $LuCl_3$ related samples) and on a Netzsch STA 449 F1 Jupiter (for $SmCl_3$ related samples). Measurements were performed on about 5 mg of sample under flowing air by heating at 10 °C/min up to 900 °C. TGA under inert atmosphere was performed using about 300 μg of sample on a TGA1 (Mettler Toledo) apparatus from 30 °C to 900 °C with a ramp of 10 °C·min^{-1} under N_2 using a flow rate of 50 mL/min and platinum pans. In this case, the estimation of the degree of functionalization by TGA was done by taking weight loss values at 650 °C, because up to 600 °C strong weight losses were still occurring. HAADF-STEM images were acquired at 20 kV on a FEI Magellan XHR 400L SEM equipped with a dedicated STEM detector. HRTEM micrographs and energy dispersive X-ray (EDX) spectra were acquired on a FEI Tecnai G2 F20 operated at 200 kV and equipped with an EDAX super ultra-thin window (SUTW) X-ray detector. Samples were dispersed in ethanol and deposited on lacey carbon Cu TEM grids (Agar).

2. Characterization of purified and filled SWCNTs by TGA

TGA of both the as-received and purified SWCNTs were performed under flowing air. Taking into account that all carbon species are oxidized to carbon dioxide, the residue after the analysis must correspond to inorganic impurities from the synthesis of the nanotubes. After TGA, the inorganic

solid residue in as-received material is 4.6 wt %, while a decrease is observed for the purified samples down to 1.7-1.9 wt %. Both, the amount of inorganic particles and amorphous carbon present in the samples of CNTs can influence the onset of the combustion temperature observed by TGA. Samples with a higher amount of inorganic material, such as metal nanoparticles, start to oxidize at lower temperatures.[3] The same trend is also observed when amorphous carbon is present because it is more easily oxidized than carbon nanotubes.[4] In agreement, the onset of the combustion temperature of the purified SWCNTs is higher than that of the as-received material, showing the higher quality of the purified nanotubes.

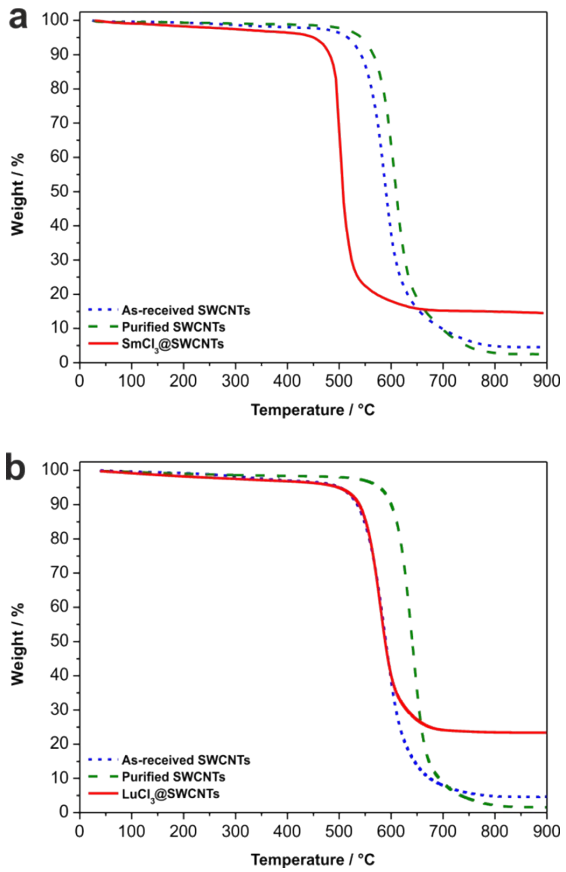

Figure S1 TGA under flowing air of (a) as-received, purified and $SmCl_3$@SWCNTs (**1a**); (b) as-received, purified and $LuCl_3$@SWCNTs (**1b**).

In the TG curves of the filled compounds (**1a** and **1b**), a decrease in the onset of the combustion temperature becomes clearly visible due to the presence of the encapsulated compounds. The filling yield of $SmCl_3$@SWCNTs (**1a**) and $LuCl_3$@SWCNTs (**1b**) corresponds to 18.1 wt % and 29.9 wt %, respectively.

3. Characterization of filled SWCNTs by HRTEM

A representative image of $LuCl_3$ confined within the cavities of carbon nanotubes is presented in Figure S2. Fast Fourier transform (Figure S2b) on the selected area confirmed the monoclinic structure of crystalline $LuCl_3$ with [001] zone axis.

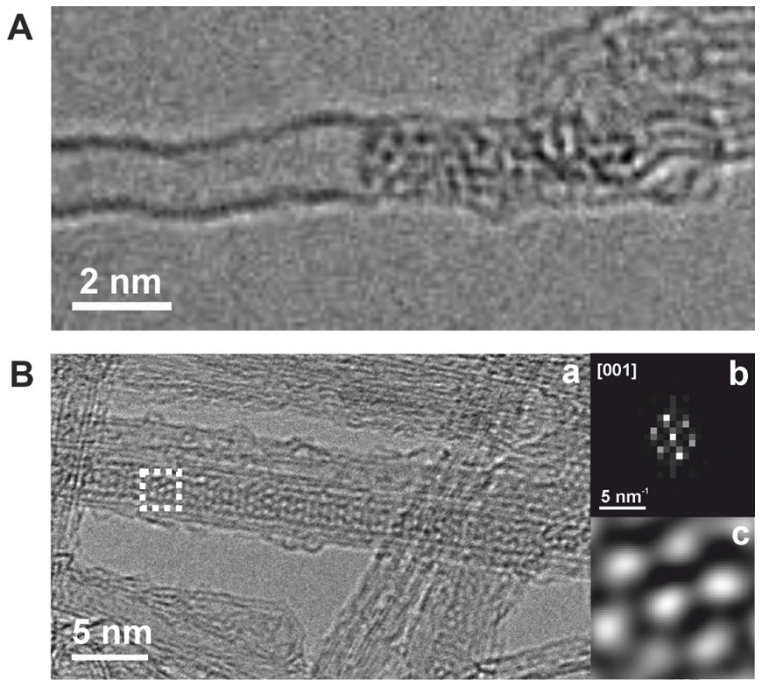

Figure S2 (A) HRTEM image of $SmCl_3$-filled carbon nanotubes. (B) (a) HRTEM image of $LuCl_3$-filled carbon nanotubes; (b) Fast Fourier transform of the white box area of the image and (c) the corresponding Inverse Fourier Transform.

4. Synthesis of the organic precursors

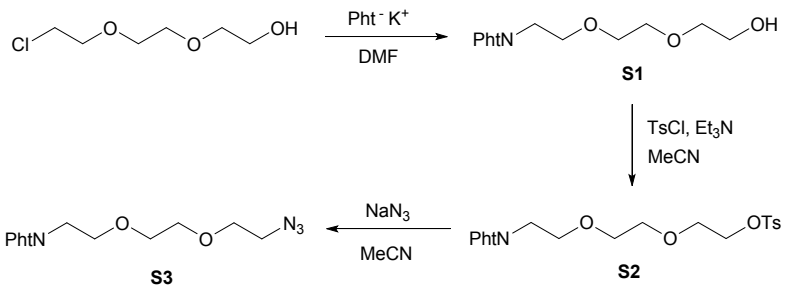

Scheme S1 Synthesis of the azide precursor **S3**.

Synthesis of N-*[2-(2-hydroxyethoxy)ethoxy]ethylphthalimide* **S1**

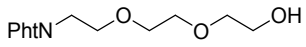

2-[2-(2-Chloroethoxy)ethoxy]ethanol (10 g, 59 mmol) was added to a solution of potassium phthalimide (12.08 g, 65 mmol) in DMF (100 mL) and stirred at 100°C for 17 h. The precipitated phthalimide salts were then removed by filtrating the solution over a celite pad. The filtrate was concentrated, diluted with H_2O (50 mL) and extracted with DCM (3x50 mL). The combined organic phases were dried over $MgSO_4$ and concentrated, affording a white viscous solid (15.7 g, 95% yield).

^{1}H NMR ($CDCl_3$, 400 MHz) δ (ppm): 7.86-7.83 (2H, m), 7.71-7.69 (2H, m), 3.90 (2H, t, *J* = 5.7 Hz), 3.75 (2H, t, *J* = 5.7 Hz), 3.66-3.59 (6H, m), 3.52 (2H, t, *J* = 4.3 Hz), 2.26 (1H, br s). All structural assignments were in agreement with previously reported data.[5]

Synthesis of N-[2-(2-tosylethoxy)ethoxy]ethylphthalimide **S2**

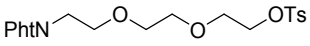

p-Toluenesulfonyl chloride (6.63 g, 34.8 mmol) was slowly added to a solution of compound **S1** (6.48 g, 23.20 mmol) and Et_3N (6.4 mL, 46.4 mmol) in MeCN (50 mL), at 0 °C and under argon. The mixture was stirred at 0 °C for 20 min and at r.t. for 1 h, and the crude was then poured into water (40 mL), extracted with EtOAc (3 x 30 mL) and dried over $MgSO_4$. The concentrated crude was further purified by flash chromatography (eluant EtOAc/cyclohexane in gradient form 1:3 to 1:1), affording **S2** as yellow oil (6.90 g, 69% yield).

^{1}H NMR ($CDCl_3$, 500 MHz) δ(ppm): 7.83-7.81 (2H, m), 7.76 (2H, d, *J* = 8.3 Hz), 7.70-7.69 (2H, m), 7.32 (2H, d, *J* = 8.3 Hz), 4.08 (2H, t, *J* = 4.8 Hz), 3.86 (2H, t, *J* = 5.8 Hz), 3.68 (2H, t, *J* = 5.8 Hz), 3.61 (2H, t, *J* = 4.8 Hz), 3.55 (2H, dd, *J* = 6.2 and 5.6 Hz), 3.51 (2H, dd, *J* = 6.1 and 5.6 Hz), 2.43 (3H, s). All structural assignments were in agreement with previously reported data.[6]

Synthesis of N-[2-(2-azidoethoxy)ethoxy]ethylphthalimide **S3**

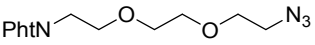

A solution of tosylate **S2** (6.9 g, 15.91 mmol) in MeCN (50 mL) was treated with NaN_3 (3.10 g, 47.75 mmol) and a catalytic amount of NaI, and refluxed (90 °C) for 48 h under argon. Because of the inherent risk related with the manipulation of azides, especially at high reaction temperatures, all manipulations were carried out with extra care using a protection screen during reaction. The cooled mixture was diluted with water (30 mL) and extracted with DCM (4 x 20 mL). The combined organic phases were dried over $MgSO_4$, concentrated and purified by flash chromatography (eluant EtOAc/cyclohexane in gradient form 1:3 to 1:2), affording the product as an orange oil (3.9 g, 80% yield).

^{1}H NMR ($CDCl_3$, 400 MHz) δ(ppm): 7.85-7.83 (2H, m), 7.72-7.70 (2H, m), 3.90 (2H, t, *J* = 5.8 Hz), 3.75 (2H, t, *J* = 5.7 Hz), 3.66-3.64 (2H, m), 3.62-3.59 (4H, m), 3.30 (2H, t, *J* = 5.1 Hz). All structural assignments were in agreement with previously reported data.[6]

5. TGA characterization of functionalized $SmCl_3$@SWCNTs

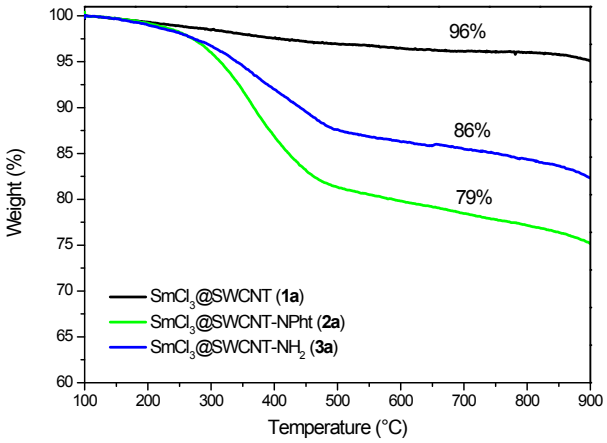

Figure S3 Thermogravimetric curves of pristine $SmCl_3$@SWCNTs (**1a**), $SmCl_3$@SWCNT-Pht (**2a**) (before deprotection) and $SmCl_3$@SWCNT-NH_2 (**3a**) (after deprotection). The percentages correspond to the weight loss observed at 650°C.

6. Derivatization with iodine tag and Z-contrast STEM imaging

In order to have a further proof of the presence of free amines on the $SmCl_3$@SWCNT-NH_2 and of their availability for further derivatization, the amino-functionalized CNTs **3a** were coupled with a 2,3,5-triiodophenyl tagging motif. The principle of *Z*-contrast STEM is that the image is strongly dependent on the atomic number (*Z*) of the observed atoms, thus a heavy-element such as iodine will appear with higher contrast compared to the carbon background of the nanotubes. In addition, the EDX detector associated with the STEM allows to obtain the elemental composition of the imaged area, providing a further characterization proof.

The 2,3,4-triiodophenyl motif was coupled to the free amine functions of $SmCl_3$@SWCNT-NH_2 (**3a**) by EDC-assisted amidation with 2,3,4-triiodobenzoic acid (Scheme S2, cf. below for experimental details). Characterization of the new conjugate by Kaiser test proved that the amount of free amines sensibly decreased, meaning that most of the amino groups have reacted with the tagging molecule and that the tag is covalently attached to the CNTs.

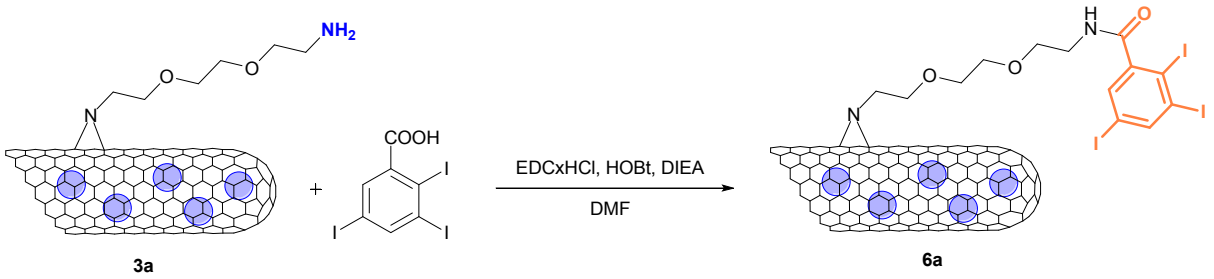

Scheme S2 Tagging of the amino groups of $SmCl_3$@SWCNT-NH_2 (**3a**) with the 2,3,4-triiodophenyl motif.

The functionalization was confirmed by TGA, comparing the thermogravimetric curves of the amino-functionalized CNTs (**3a**) with that of the tag-functionalized CNTs (**6a**) (Figure S3). The weight loss corresponding to $SmCl_3$@SWCNT-I (**6a**) is higher than that of the aminated precursor (**3a**), as expected, since there is an increase in molecular weight upon reaction.

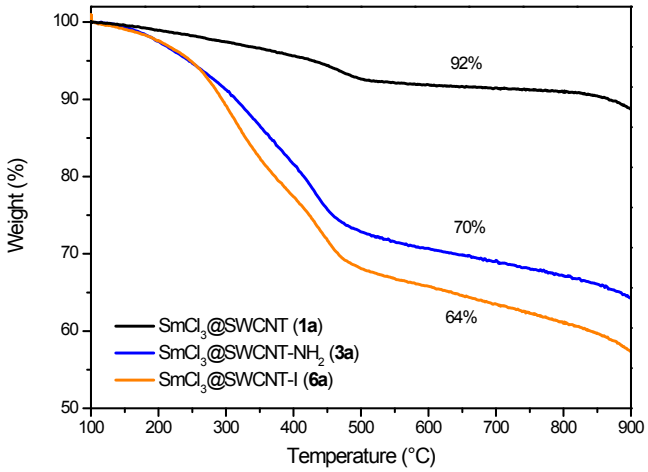

Figure S4 TG curves of pristine $SmCl_3$@SWCNTs (**1a**), amino-functionalized CNTs (**3a**) and tag-functionalized CNTs (**6a**). The percentages correspond to the weight loss observed at 650°C.

The obtained $SmCl_3$@SWCNT-I (**6a**) were further characterized by high-resolution STEM and EDX. By microscopy imaging it was possible to visualize many randomly distributed bright dots along the CNT sidewalls, which were not observed in the amino-functionalized CNT precursor (**3a**) (Figure S5). These bright dots were attributed to the iodine atoms of the tag molecule, and the elemental analysis of specific imaged areas performed by EDX gave a further proof of the

presence of iodine (Figure S6). By both STEM and EDX of compound **6a** it was possible to simultaneously detect the filling material (samarium chloride) and the external iodine tag.

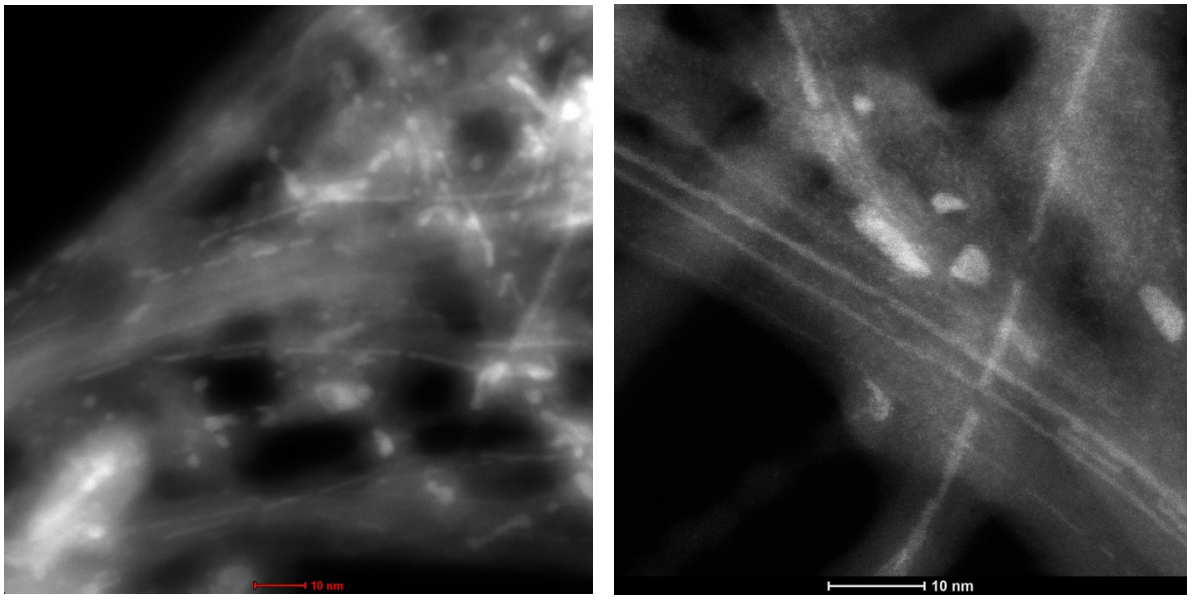

Figure S5 Simultaneous detection of filling and functionalization. *Z*-contrast STEM images of $SmCl_3$@SWNT-NH_2 (**3a**) (left) and $SmCl_3$@SWNT-I (**6a**) (right). The bright rods correspond to the filling material ($SmCl_3$), while the tiny bright dots on the right-side image are generated by the iodine atoms.

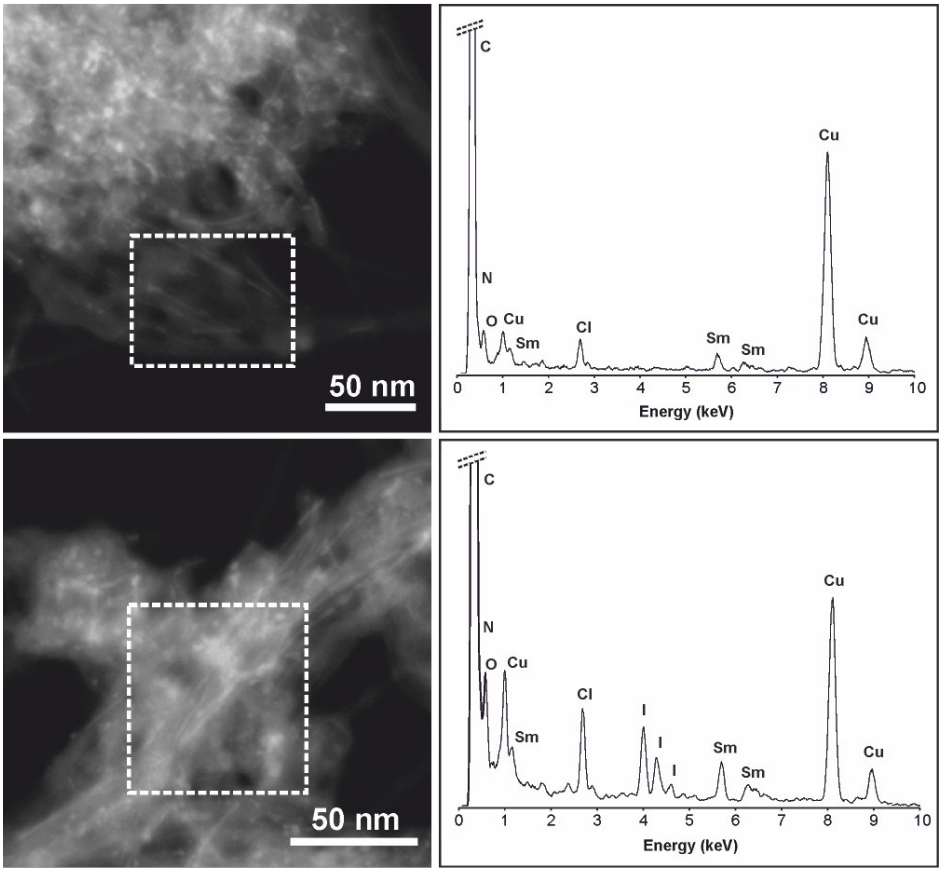

Figure S6 HAADF STEM images of conjugates **3a** (top) and **6a** (bottom) and the corresponding EDX analyses on the areas marked by the dotted squares.

Experimental details for the synthesis of iodinated SWCNT conjugate

In a flame-dried Schlenk tube, pristine $SmCl_3$@SWCNTs (**1a**) (10 mg) were dispersed in dry NMP (8 mL) by sonicating for 15 min under argon. A solution of azide **S3** (200 mg) in dry NMP (2 mL), was added to the CNT dispersion by syringe, and the mixture stirred at 200 °C for 12 h, under argon. The cooled mixture was then diluted with EtOH (20 mL) and filtered (0.1 μm). The CNTs recovered on the filter were washed by dispersing them in DMF (20 mL), sonicating for 10 min and filtrating. This washing sequence was further repeated with MeOH (x 2) and with acetone (x 2). The CNTs were then dialyzed against ddH_2O for 2 days and lyophilized.

The cleavage of the phthalimide group was carried out as described in the main paper, finally obtaining 8 mg of $SmCl_3$@SWCNT-NH_2 (**3a**). The amine loading determined by Kaiser test is 204 μmol/g.

Amino-functionalized CNTs **3a** (5 mg) were dispersed in dry DMF (5 mL) by sonicating for 30 min. 2,3,4-Triiodobenzoic acid (100 mg, 20 eq. w/w, 0.2 mmol), HOBt (54 mg, 0.4 mmol) and DIEA (0.25 mL, 5% v/v) were then added to the dispersion at r.t., and finally EDCxHCl (154 mg, 0.8 mmol) was added at 0 °C. The mixture was briefly sonicated and then stirred at r.t. for 48 h. After

filtration, the recovered CNTs were washed with DMF (x 2), MeOH (x 2) and acetone (x 1), and finally dried *in vacuo*. From the Kaiser test, the amount of free amine results to be 34 μmol/g, corresponding to a conversion yield of 83%.

7. Examination of EGFR expression by Western blot analysis

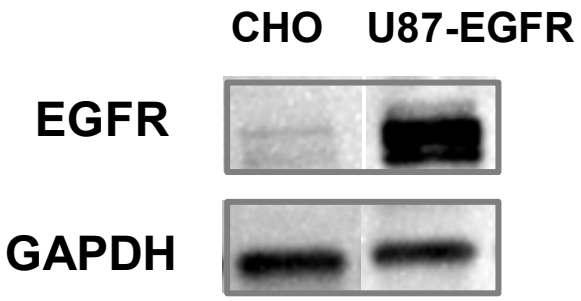

Figure S7 Western blot analysis of EGFR protein expression from CHO and U87-EGFR+ cells. The expression of EGFR protein in U87-EGFR+ was confirmed by Western blot analysis. Relatively lower EGFR expression was detected from CHO cells. The GAPDH antibody was used as an internal control.

8. Uptake-Mean Fluorescence Intensity of functionalized $SmCl_3$@SWCNTs 3a, 4a and 5a

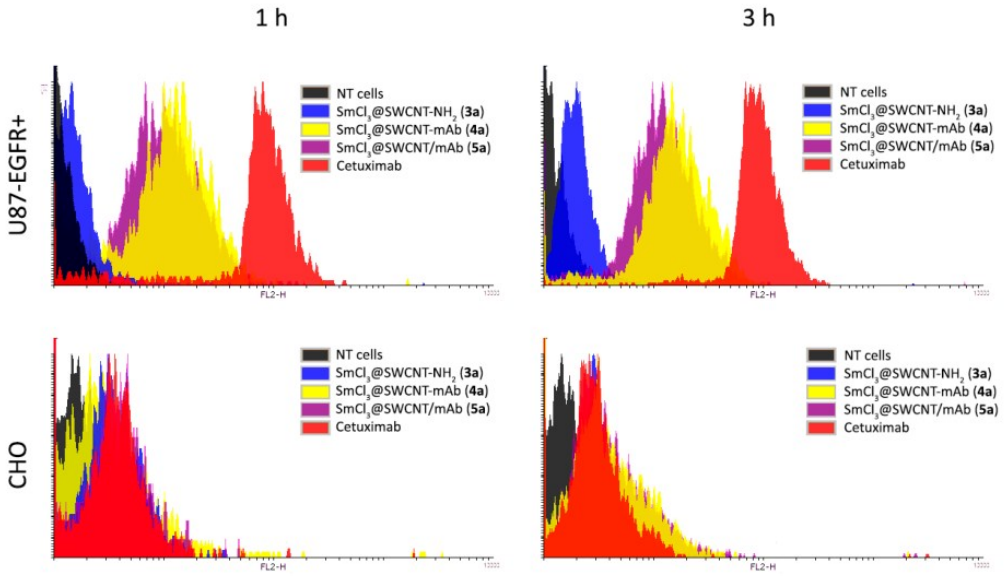

Figure S8 Histograms representing the fluorescence intensity of cells after 1 or 3 hours treatment with $SmCl_3$@SWCNT-NH_2 (**3a**), $SmCl_3$@SWCNT-mAb (**4a**) and $SmCl_3$@SWCNT/mAb (**5a**). The more the histogram is shifted to the right, the higher the amount of Cetuximab within the cells. NT: Non treated cells.

9. Cytotoxicity study of functionalized $SmCl_3$@SWCNTs

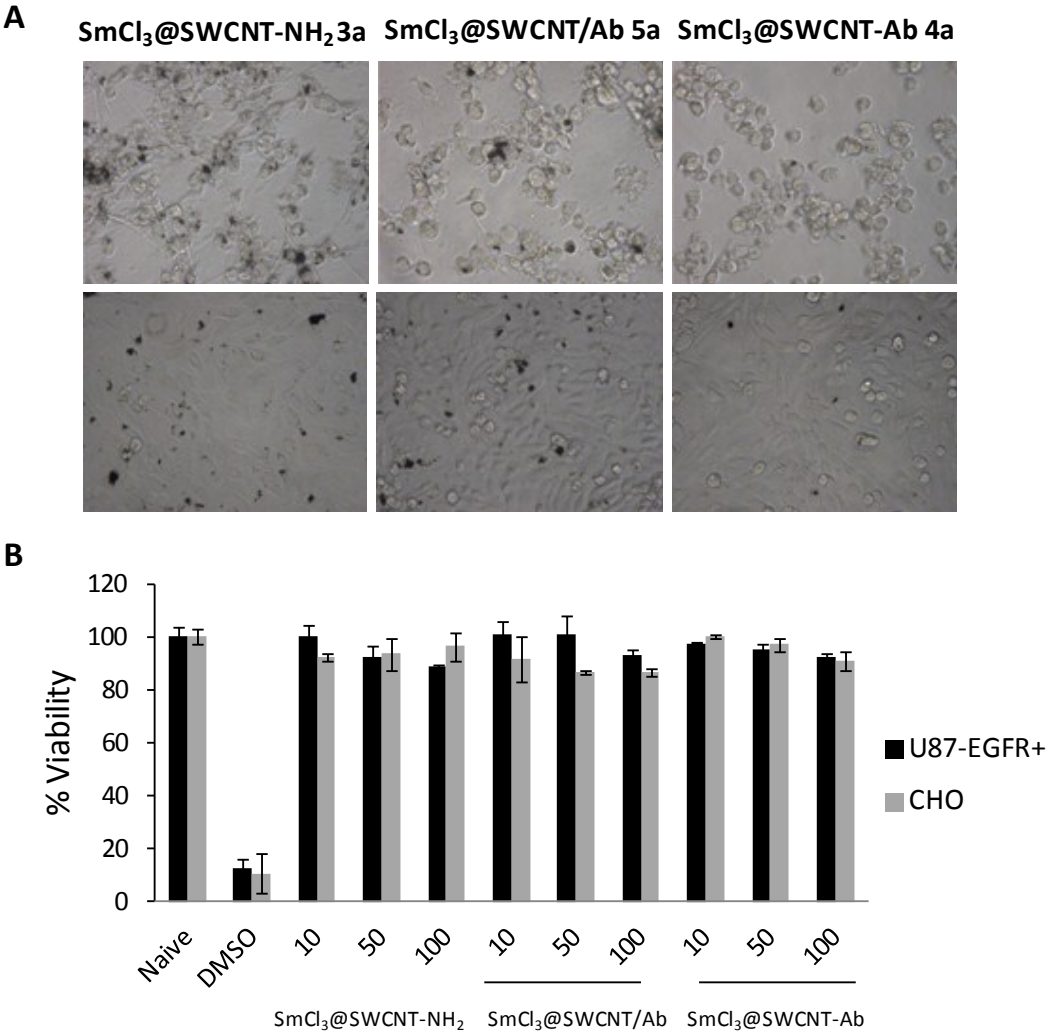

Figure S9 Cytotoxicity of CNTs in U87-EGFR+ and CHO cells *in vitro*. Cells were incubated with CNTs for 24 h at increasing concentrations (10, 50 and 100 µg/mL). A) Microscopic examination of cells after treatment with CNTs for 24 h. B) Cell viability was quantified as intracellular LDH content and no significant changes were observed for all compounds after 24 h of incubation (n = 3). Values are expressed as mean ± SD.

10. Fluorescent labeling of Cetuximab

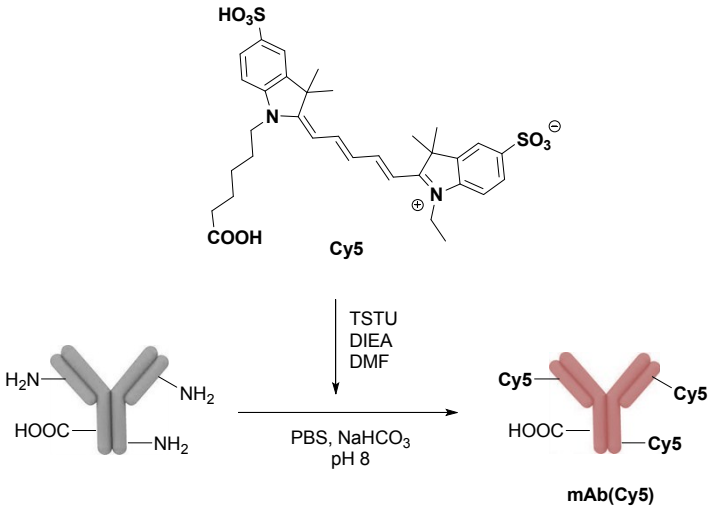

Scheme S3 Multi-labeling of Cetuximab with Cy5.

Formula for the determination of the degree of labeling (DL):

$$DL = \frac{A_{650} \times \varepsilon_{280}}{(A_{280} - A_{650} \times CF) \times \varepsilon_{650}}$$

where: A_{280} and A_{650} = absorbance of the conjugate solution at 280 nm and 650 nm

CF = correction factor due to the contribution of the dye at 280 nm (0.05)

ε_{280} = molar extinction coefficient of the antibody (203000 $cm^{-1} \cdot M^{-1}$)

ε_{650} = molar extinction coefficient of the dye (250000 $cm^{-1} \cdot M^{-1}$)

11. Conjugation of mAb(Cy5) to $LuCl_3$@SWCNT-NH_2 (3b)

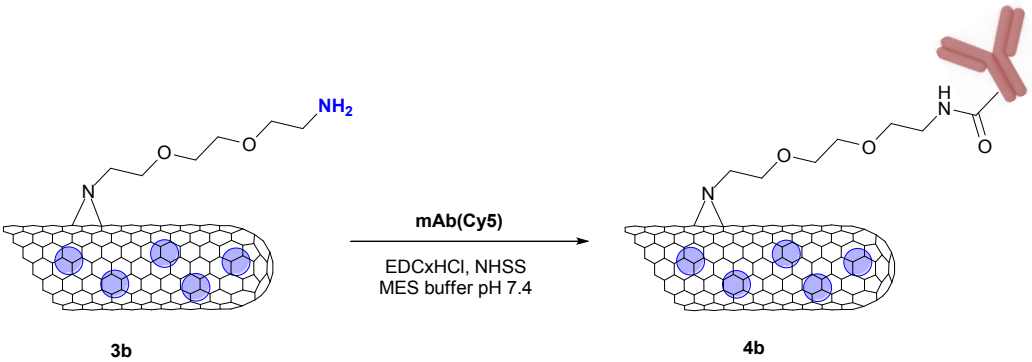

Scheme S4 Covalent derivatization of $LuCl_3$@SWCNT-NH_2 (**3b**) with the labeled Cetuximab [mAb(Cy5)].

12. Characterization of functionalized $LuCl_3$@SWCNTs by TGA

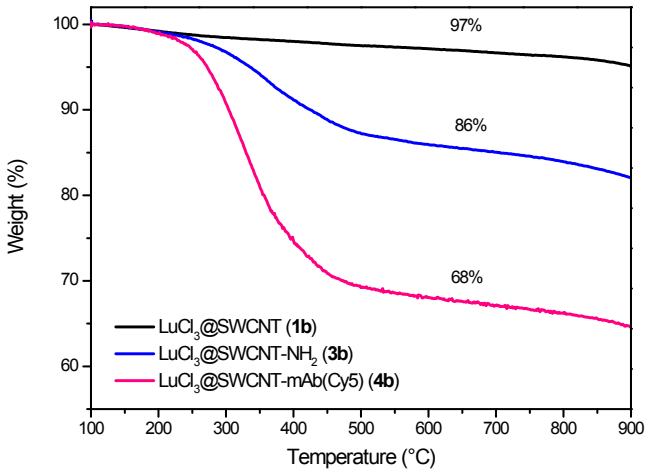

Figure S10 Thermogravimetric curves of $LuCl_3$@SWNTs (**1b**), amine-functionalized SWCNTs **3b** and antibody functionalized SWCNTs **4b**. The percentages correspond to the weight loss observed at 650°C.

13. Characterization of $LuCl_3$@SWCNT-mAb(Cy5) (4b) by gel electrophoresis

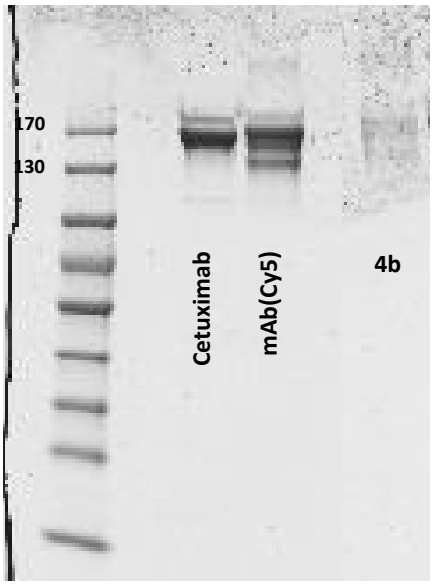

Figure S11 Gel electrophoresis of Cetuximab, labeled-Cetuximab [mAb(Cy5)] and $LuCl_3$@SWCNT-mAb(Cy5) (**4b**) run under non-reducing conditions at 150 V. Gel stained with Coomassie blue. Protein size marker on lane 1 (size in kDa).

14. Uptake-Mean Fluorescence Intensity of $LuCl_3$@SWCNT-mAb(Cy5) (4b)

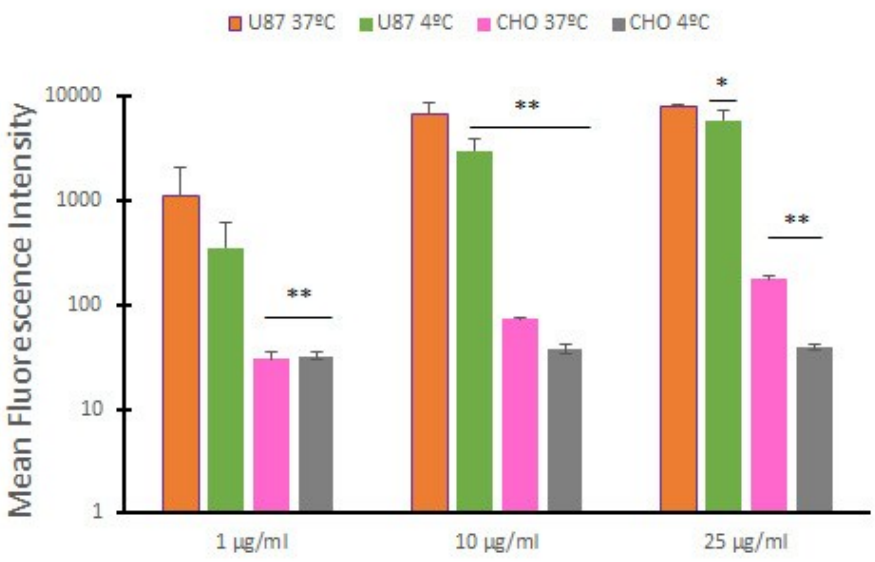

Figure S12 Bars representing the mean fluorescence intensity of the same cells using 1, 10 or 25 µg/ml of $LuCl_3$@SWCNT-mAb(Cy5) (**4b**). Error bars represent the SD (n=3). *p>0.05, **p<0.01 Vs. U87 at 37 °C.

15. REFERENCES

1. E. Kaiser, R. L. Colescott, C. D. Bossinger, and P. I. Cook, *Anal. Biochem.*, 1970, **34**, 595–598.

2. C. Samorì, R. Sainz, C. Ménard-Moyon, F. M. Toma, E. Venturelli, P. Singh, M. Ballestri, M. Prato, and A. Bianco, *Carbon*, 2010, **48**, 2447–2454.

3. B. Ballesteros, G. Tobias, M. A. H. Ward, and M. L. H. Green, *J. Phys. Chem. C*, 2009, **113**, 2653–2656.

4. R. Brukh and S. Mitra, *J. Mater. Chem.*, 2007, **17**, 619–623.

5. H. Sato, E. Hayashi, N. Yamada, M. Yatagai, and Y. Takahara, *Bioconjugate Chem.*, 2001, **12**, 701–710.

6. G. Lu, S. Lam, and K. Burgess, *Chem. Commun.*, 2006, 1652–4.